1 **Experimental determination of zinc isotope fractionation in complexes with**

2 **the phytosiderophore 2'-deoxymugeneic acid (DMA) and its structural**

3 **analogues, and implications for plant uptake mechanisms**

4

5

6 [a]Tamara Marković, [a]Saba Manzoor, [b]Emma Humphreys-Williams, [c]Guy JD Kirk, [d]Ramon Vilar,

7 [a,f,]*Dominik J Weiss

8

9

10 [a]Department of Earth Science & Engineering, Imperial College London, London SW7 2AZ, United

11 Kingdom, current affiliation

12 [b]Core Research Laboratory, Natural History Museum London, SW7 5BD, United Kingdom

13 [c]School of Water, Energy & Environment, Cranfield University, Cranfield, Bedford MK43 0AL,

14 United Kingdom

15 [d]Department of Chemistry, Imperial College London, London SW7 2AZ, United Kingdom

16 [f]Stanford School for Earth, Energy and Environmental Sciences, Stanford University, Stanford CA

17 94305, United States of America

18

19 *Corresponding author: d.weiss@imperial.ac.uk, tel. +44 20 7594 6383

20

ABSTRACT

The stable isotope signatures of zinc are increasingly used to study plant and soil processes. Complexation with phytosiderophores is a key process and understanding the controls of isotope fractionation is central to such studies. Here, we investigated isotope fractionation during complexation of Zn^{2+} with the phytosiderophore 2'-deoxymugeneic acid (DMA) - which we synthesised - and with three commercially-available structural analogues of DMA: EDTA, TmDTA and CyDTA. We used ion exchange chromatography to separate free and complexed zinc, and identified appropriate cation exchange resins for the individual systems. These were Chelex-100 for EDTA and CyDTA, Amberlite CG50 for TmDTA and Amberlite IR120 for DMA. With all the ligands we found preferential partitioning of isotopically heavy zinc in the complexed form, and the extent of fractionation was independent of the Zn:ligand ratio used, indicating isotopic equilibrium and that the results were not significantly affected by artefacts during separation. The fractionations (in ‰) were $+0.33 \pm 0.07$ (1σ, n=3), $+0.45 \pm 0.02$ (1σ, n=2), $+0.62 \pm 0.05$ (1σ, n=3) and $+0.30 \pm 0.07$ (1σ, n=4) for EDTA, TmDTA, CyDTA and DMA, respectively. Despite the similarity in Zn-coordinating donor groups, the fractionation factors are significantly different and extent of fractionation seems proportional to the complexation stability constant. The extent of fractionation with DMA agreed with observed fractionations in zinc uptake by paddy rice in field experiments, supporting the possible involvement of DMA in zinc uptake by rice.

INTRODUCTION

With the introduction of multi-collector inductively coupled plasma mass spectrometry (MC-ICP-MS), it has become possible to measure stable-isotope fractionation of metals in natural systems in the way that is routinely done for light elements such as C, O, N, and S [1]. Isotope systems are now available to study biogeochemical processes controlling trace element cycling in the natural environment. Of special interest are applications to study metal cycling in soil environments and during plant uptake, as mediated by rhizosphere processes. To date, complex root-soil interactions have only been studied indirectly using experiments in artificial laboratory systems or using mathematical modelling. The lack of direct techniques without artificial manipulations has hampered progress. Isotope fractionation at natural abundance has much to offer in this. Recent work has shown significant isotope fractionations in trace element uptake by plants, as well as differences between plant species, likely reflecting different uptake mechanisms [2].

In previous work on zinc uptake un rice, we found a light isotope bias in experiments conducted with solution cultures [3] but a neutral or heavy isotope bias in zinc uptake by rice grown in soils under aerobic and anaerobic conditions and with different zinc status [4, 5]. This is suggesting that uptake mechanisms in rice are controlled by environmental factors. Indeed, studies with other plant types (hyper-accumulators and non-accumulators, grasses, trees) showed equally a neutral or heavy isotope bias during zinc uptake when grown in soils [6-9] and a light isotope bias in studies when grown in hydroponic solutions [10-12].

Different processes have been proposed to explain the observed isotope patterns including zinc uptake from different soil pools [6] and the involvement of Zn-chelating phytosiderophores. The latter mechanism has been invoked because a heavy bias is expected in equilibrium fractionation during

61 ligand formation [13]. Indeed, Guelke and von Blankenburg (2007) found a heavy isotope bias in iron
62 uptake by grass species, which are known to secrete phytosiderophores to facilitate iron uptake; but a
63 light isotope bias in iron uptake by non-grass species, which do not secrete phytosiderophores [14].

64   It has been speculated that phytosiderophores are involved in the solubilisation and uptake of soil
65 zinc by rice, as well as in its transport within the plant [4, 15-17]. To assess if observed isotope patterns in
66 rice are possibly linked to Zn-chelating phytosiderophores, there is a need to constrain the equilibrium
67 isotope fractionation during the complexation of zinc with phytosiderophores. However, there are
68 significant experimental and analytical challenges to this. First, the phytosiderophore studied needs to
69 be in a very pure state to avoid interferences during complexation. Isolates from plants and root
70 secretions are prone to impurities [18]. It is preferable to synthesise the phytosiderophore. Protocols for
71 the multi-step synthesis of the phytosiderophore DMA have been reported [19, 20], making DMA a
72 suitable model phytosiderophore to study zinc fractionation. Second, there is the considerable
73 challenge of separating free and complexed species from aqueous solutions without inducing artificial
74 isotope fractionation [21, 22]. The only previous attempt to do this for isotope fractionation studies of Zn-
75 organic ligand complexation used a Donnan membrane [23]. Use of Donnan membranes, however, is
76 time consuming, prone to blank contributions due to the numerous steps involved, and there are
77 possible implication of slow dissociation of metals [24]. Ion exchange chromatography can avoid these
78 problems if suitable resins can be found as successfully demonstrated for iron [22]. The ion-exchange
79 properties of potential resins can be predicted from the protonation and complexation constants of the
80 resin's hydro-soluble active groups in aqueous solution. However, sorption of divalent metal ions on
81 resins does not take place through simple ion exchange, and so the separation of free and complexed
82 species is not easily predictable from the resin's ion-exchange properties alone [25]. To determine
83 equilibrium isotope fractionation, there should be no exchange of zinc between the complex and
84 exchange resin. One widely used approach to test this is to determine the isotope fractionation
85 between reactants and products using a range of metal:ligand ratios [21, 26, 27]. The net isotope
86 fractionation must be independent of the metal:ligand ratio within analytical precision. Other methods
87 include the use of isotope spikes [21, 22] but these are prone to issues such as equilibration rates.

88   Given these challenges, experimental studies of isotope fractionation between metal cations and
89 organic ligands are limited. Jouvin and colleagues[23] investigated the isotopic fractionation during
90 adsorption onto purified humic acid (PHA) and found that zinc bound to PHA was isotopically heavier
91 than free Zn^{2+} ($\Delta^{66}Zn_{ZnPHA-freeZn2+}$ = 0.24 ± 0.06). The fractionation factor depended on the affinity of
92 the sites and on the pH of the solution. Using humic acids to improve our understanding of the
93 underlying physical-chemical controls of isotope fractionation, however, has the disadvantage that
94 they are structurally poorly constrained and hence a systematic investigation of structural controls (i.e.
95 numbers of donors such as nitrogen, oxygen, the effect of the denticity, ligand affinity etc.) is not
96 possible. Experimental studies involving other transition metals were conducted with iron and
97 desferrioxamine B (DFOB) [21, 22], EDTA and oxalate [22] and with copper and insolubilized humic acid
98 (IHA) [28], ethylendiaminetetraacetic acid (EDTA), nitrotriacetic acid (NTA), iminodiacetic acid (IDA)
99 and DFOB [29]. These experimental studies found all a preference for the heavy isotope during
100 complexation and structural controls including complexation strength and bond distances were put
101 forward as possible controls.

102   The goal of the present study was to determine for the first time isotopic fractionation factors for
103   zinc complexation by a natural phytosiderophore, i.e., DMA, and structurally similar polydentate
104   ligands. We synthesised DMA using recently published methods, and we identified the best resins to
105   separate free and complexed Zn^{2+} for the ligands under study. We then determined the direction and
106   extent of isotopic fractionation during complexation at different Zn:ligand ratios, and tested for
107   possible controls such as ligand affinity and bonding environment.

108   **MATERIALS AND METHODS**

109   **Choice of ligands.** We chose DMA since it has been proposed to play a major role in zinc uptake in
110   rice. There is a good synthetic protocol to prepare pure samples of DMA in good yields, therefore
111   from a practical point of view it is possible to get pure sample material.   We chose
112   ethylenediaminetetraacetic acid (EDTA), trimethylenedinitrilotetraacetic acid (TmDTA) and
113   cyclohexanediaminetetraacetic acid (CyDTA) as additional ligands because they are commercially
114   available, hexadentate ligands (like DMA) that bind zinc with high affinities giving complexes with
115   the same overall geometry and coordination sphere as DMA – i.e. all the complexes are octahedral and
116   they all use the same donor atoms to coordinate zinc: 4 oxygens and 2 nitrogens (Figure 1).

117   **Synthesis of DMA.** We used synthesis protocols previously published [19, 20]. Details are given in
118   the Supporting Information. All starting materials and reagents were purchased from commercial
119   sources and used without further purification. The progress of the synthesis was monitored by ^{1}H
120   NMR spectroscopy at 297 K in the solvent indicated, using a Bruker AC300 spectrometer. The spectra
121   were calibrated with respect to tetra-methylsilane and the residual solvent peaks indicated in the
122   relevant spectrum.

123   **Choice of resins.** Three resins were assessed based on their suggested abilities to sequester free
124   Zn^{2+} without interacting with the Zn-ligand complex. The resins were Chelex-100 (BioRad, Na^+ form,
125   100–200 mesh, containing carboxyl functional groups) for the complexes with EDTA and CyDTA [30],
126   Amberlite CG50 (Dow, H^+ form, 100–200 mesh, also containing carboxyl functional groups) for the
127   complexes with TmDTA [25, 30], and Amberlite IR120 (Alfa Aesar, H^+ form, containing sulfonic acid
128   functional groups) for the complexes with DMA [18].

129   **Preparation of solutions.** All solutions were prepared in Teflon Savillex vials (Savillex, MN,
130   USA). Acid solutions were prepared using 18 MΩ-grade Millipore water (Bedford, MA, USA) and
131   AnalaR grade HCl (6 M) and HNO_3 (15.4 M), both sub-distilled. Stock solutions were prepared as
132   follows: 1 mM $Zn(OAc)_2$ at pH 6.2 by dissolving $Zn(OAc)_2$ dihydrate (0.11 g) in 500 ml of MQ H_2O;
133   and 1 mM Na_4EDTA by dissolving Na_4EDTA dihydrate (0.095 g) in 250 ml of MQ H_2O and heating
134   at 60°C until complete dissolution. Similarly, 250 ml of 1 mM stock solutions of TmDTA (0.077 g)
135   and CyDTA monohydrate (0.091 g) were prepared. Potassium 2-(*N*-morpholino)ethanesulfonic acid
136   (KMES) buffer solution (0.5 M) was prepared by dissolving MES monohydrate (26.66 g) in 250 ml of
137   Millipore H_2O and stirring at 60 °C until complete dissolution was achieved. The pH of the solution
138   was adjusted to 6.2 by the addition of 3 M KOH aqueous solution. $Zn(OAc)_2 \cdot 2H_2O$, CyDTA
139   monohydrate and TMDTA were purchased from Sigma-Aldrich, Na_4EDTA from Fisher Scientific and
140   MES monohydrate from VWR.

141   Different ratios (mol:mol) of free Zn^{2+} to complexed ZnL^{2-} were prepared by adding 10 ml of 1
142   mM $Zn(OAc)_2$ to a corresponding volumes of 1 mM ligand solution. All reagents were prepared using

143   18.2 mΩ cm Millipore water.   The solutions were buffered to pH 6.2 using 0.5 M KMES and
144   equilibrated overnight before proceeding to the ion exchange separation. Although all weighing was
145   done gravimetrically, some error in molar quantities is possible for the ligand compounds due to their
146   hygroscopic character.   We confirmed that complete complexation was reached upon mixing
147   equimolar solutions of $Zn(OAc)_2$ and L^{4-} where L^{4-} refers to the deprotonated ligand at pH 6.2 using
148   GEOCHEM-EZ software [31].

149   Commercial solutions of Cu (ROMIL Ltd, Cambridge, UK) and Zn (ROMIL Ltd, Cambridge,
150   UK) were used as dopant solution for instrumental mass bias correction and for quality control of the
151   isotope measurement on the MC-ICP-MS, respectively [32].

152   **Ion exchange procedures.** We adapted two previously published ion exchange protocols: a
153   cation exchange procedure for the separation of free and complexed zinc [33] and an anion exchange
154   procedure for the separation of zinc fractions from the Na-rich solution matrix for subsequent isotope
155   ratio measurements [34]. The protocol of these procedures is shown in Table 1. All resins were prepared
156   and cleaned according to the manufacturers' recommendations and loaded onto BioRad PolyPrep
157   columns. In general, the resin was soaked in 100 ml of Millipore H_2O per 5 g of resin, and then
158   pipetted into BioRad Poly-Prep (Bio-Rad Laboratories, CA, USA) columns (i.d. 8 mm). The resin
159   was cleaned with 2 M HCl and equilibrated with 0.5 M KMES buffer (pH 6.2). The buffered samples
160   were loaded on to the column. The Zn-ligand complex was collected straight away as the samples ran
161   down the column. The resin was further equilibrated with the buffer to elute any remaining complexed
162   zinc. Washing the column with 1M HCl eluted all free Zn^{2+} initially ex-changed with the resin matrix.
163   After collecting both free and complexed zinc, the fractions were evaporated to dryness and refluxed
164   in 15.6 M HNO_3 at 100 °C for 3 h prior to drying at 120 °C to remove the easily oxidisable organic
165   ligand material. After final drying, the samples were re-dissolved in 0.3 M HNO_3 for concentration
166   measurements.

167   All collected samples, containing free Zn^{2+} or digested Zn-ligand complex, were evaporated to
168   dryness, refluxed in 5.8 M HCl, diluted in 1 ml of 5.8 M HCl and passed through PolyPrep columns
169   containing 0.7 ml AG-MP1 resin (Bio-Rad, Cl⁻ form, 100–200 mesh) anion-exchange resin, before
170   evaporation and reflux in 15.6 M HNO_3. Evaporated samples were re-dissolved in 0.5 M HNO_3. The
171   fractions containing Zn-ligand complexes were dissolved in a mixture of 5 ml 15.6 M HNO_3 and 3 ml
172   30% (v/v) H_2O_2, and digested using a microwave oven (210 °C, 1.7 kPa, 90 min) to break down the
173   organic matrix [35]. All experimental work associated with preparation of samples and ion exchange
174   chromatography was carried out in Class 10 laminar flow hoods in a Class 1000 Clean Laboratory.

175   **Zinc concentration and isotopic composition measurements.**   Zinc concentrations were
176   determined using ICP-AES (Thermo iCap 6500 Duo, Thermo Scientific, UK). Zinc isotope ratios
177   were measured using multi collector ICP-MS (Nu Plasma, Nu Instruments, UK) and are expressed
178   using the conventional $\delta^{66}Zn$ notation (‰):

179    $\delta^{66}Zn = (({}^{66}Zn/{}^{64}Zn)_{sample} / ({}^{66}Zn/{}^{64}Zn)_{standard} - 1) \times 1000$ (1)

180   The empirical external normalisation method [32] was used to correct for instrumental mass bias and the
181   measurements were bracketed with the in-house standard London Zn. Accuracy and precision of the
182   isotope measurements were assessed by analysing two single element solutions during each
183   measurement session: IRMM 0072 and Romil Zn [36]. The results were $\delta^{66}Zn_{IRMM} - \delta_{66}Zn_{London}$ = -0.25

184    $\pm$ 0.07 ‰ (2 SD, n = 6) and $\delta^{66}Zn_{Romil} - \delta^{66}Zn_{London}$ = -9.00 $\pm$ 0.06 ‰ (2 SD, n = 6). These $\delta^{66}Zn$ values

185   agree well with previously published values [36].

186   For every ligand system tested, the $\delta^{66}Zn$ values of the initial solution (i.e. $Zn(OAc)_2$) and of the

187   free and complexed zinc fractions were determined. To quantify the isotope effect caused by

188   complexation of zinc with the test ligands, the isotopic fractionation was calculated as:

189         $\Delta^{66}Zn_{ZnL2- - Zn2+} = \delta^{66}Zn_{ZnL2-} - \delta^{66}Zn_{Zn2+}$ (2)

190   , where L refers to the tested ligand.

191   The isotope value for the complexed zinc fraction was also calculated using mass balance

192   constraints to test the integrity of the data as organic containing samples are well known to be difficult

193   for precise and accurate isotope ratio measurements:

194         $\delta^{66}Zn_{system} = (\delta^{66}Zn_{Zn2+}.f_{Zn2+}) + (\delta^{66}Zn_{ZnL2-}.f_{ZnL2-})$ (3)

195   , where $\delta^{66}Zn_{system}$ is the isotope composition of the initial solution, $\delta^{66}Zn_{Zn2+}$ and $\delta^{66}Zn_{ZnL2-}$ are the

196   isotope values of the free and of the complexed Zn fraction, respectively, and f_{Zn2+} and f_{ZnL2-} are the

197   mol fractions of free and of complexed Zn fractions calculated as $f_x = m_{fraction} / m_{total}$.

198   **RESULTS AND DISCUSSION**

199   **Separation of free and complexed zinc using cation exchange chromatography.** We

200   confirmed using GEOCHEM-EZ [31] that complete complexation was reached upon mixing equimolar

201   solutions of $Zn(OAc)_2$ and L^{4-}, where L^{4-} refers to the deprotonated ligand at pH 6.2, and that no other

202   complexes were formed. Table 2 shows the separation performance of the resins with respect to the

203   different Zn^{2+}/ZnL^{2-} systems studied in this work. Chelex-100 shows quantitative recovery and

204   separation within 5% of the prepared mol fractions of free Zn^{2+} and $ZnEDTA^{2-}$ and $ZnCyDTA^{2-}$

205   complexes. EDTA and CyDTA were the ligands used with the highest affinity for zinc(II), i.e. with

206    $\log K$ = 16.4 and $\log K$ = 18.5, respectively [37]. In contrast, Chelex-100 is too strong for the

207    $ZnTmDTA^{2-}$ complex ($\log K$ = 15.6) and we observe partial dissociation of the complex leading to an

208   increased mol fraction of Zn^{2+}/Zn_{total} in the eluent (Table 2). However, we found good separation in

209   line with the mol fractions prepared for free Zn^{2+} and $ZnTmDTA^{2-}$ using Amberlite CG50. With

210   respect to DMA ($\log K$ = 12.8), we found a slight difference between the initial molar fraction and the

211   measured one (Table 2). Although all weighing was done gravimetrically, there is inevitably some

212   variability in the molar quantities of DMA due to its hygroscopic character. Other possible processes

213   which could affect the molar fractions for the $Zn^{2+}/ZnDMA^{2-}$ in the starting solution are shifts in pH,

214   complexation with the resin or effects of the matrix [25]. The differences between targeted and real mol

215   fractions, however, did not affect the isotope fractionation (see discussion below), suggesting that

216   dissociation from the resin was not the controlling process.

217   Figure 2 shows the elution sequence of the $Zn^{2+}/ZnCyDTA^{2-}$ system. The zinc complexes are

218   eluted from the corresponding resin during the sample loading process in H_2O and the subsequent

219   matrix elution step using KMES buffer, whereas free Zn^{2+} is retained and only eluted on addition of 1

220   M HCl. Figures 2a to 2c show the elution profiles for three samples of the $Zn^{2+}/ZnCyDTA^{2-}$ system

221   with different molar ratios of free Zn^{2+} to total Zn. With no free Zn^{2+}, the ZnL^{2-} complex is eluted

222   instantly and no further zinc is recovered upon elution with 1 M HCl. For the 0.5 mol fraction of free

223   Zn^{2+}, the complexed ZnL^{2-} fraction is eluted during the sample loading and buffer elution steps, while

224   the free Zn^{2+} is eluted with 1 M HCl. Finally, for the solution with only free Zn^{2+}, no Zn^{2+} is eluted

225   during the initial two steps (sample loading and matrix elution with the buffer solution, Table 2),
226   whereas upon addition of 1 M HCl, elution of free Zn^{2+} was instantaneous, explaining the sharp peak
227   after 24 ml following the change to the 1M HCl solution (Figure 2a). Between 96 and 105 % of the
228   zinc was recovered in all test conducted and shown in Table 2.
229   **Isotope fractionation during complexation reactions.**   Table 3 shows the isotope ratios
230   (expressed using the $\delta^{66}Zn$ notation) of the free Zn^{2+} fraction (experimentally determined) and of the
231   complexed zinc fraction (experimentally determined and calculated based on mass balance, see
232   equation 3) for the four different ligands (DMA, EDTA, CyDTA, TmDTA) systems and for different
233   mol fractions. Also shown is the recovery of zinc, i.e. zinc loaded onto the column vs zinc eluted. In
234   general, we obtained a very good recovery in all of them. Only experiments where measured and
235   calculated values for $\delta^{66}Zn_{ZnL2-}$ agreed within the reproducibility of the isotope ratio determinations
236   were considered for further evaluation, guaranteeing an internally consistent data set.
237   As seen in Table 3, we found that the heavier isotope is preferred in the complexed zinc in all four
238   ligand systems investigated during the course of this study (Table 3). The preferential accumulation of
239   the heavy isotope in the ZnL^{2-} complexes is in agreement with equilibrium reaction dynamics on
240   formation of strong bonds between metals and ligands [13]. The magnitude of isotope fractionation
241   between free and complexed zinc (expressed as $\Delta^{66}Zn_{ZnL2- - Zn2+}$, Equation 2) are within error for the
242   different mol fractions studied in each system. Theory predicts that if a closed system is at isotopic
243   equilibrium, then the Δ-value will be independent of the mol fraction [38]. The fractionation factors
244   determined in this study are therefore at thermodynamic equilibrium. Dissociation of the ZnL^{2-}
245   complex on the resins, including for the $Zn^{2+}/ZnDMA^{2-}$ system, is thus unlikely or at least insignificant
246   as discussed above. The average values for $\Delta^{66}Zn_{ZnL2- - Zn2+}$ are +0.33 ± 0.07 ‰ (1σ, n = 3) for
247   $ZnEDTA^{2-}$, +0.45 ± 0.02 ‰ (1σ, n = 2) for $ZnTmDTA^{2-}$, +0.62 ± 0.05 ‰ (1σ, n = 3) for $ZnCyDTA^{2-}$,
248   and +0.30 ± 0.07 ‰ (1σ, n = 4) for $ZnDMA^{2-}$.
249   Table 4 gives a compilation of selected fractionation factors normalised per atomic mas unit for
250   the complexation of transition row metals (Fe, Zn, Ni and Co) with organic ligands derived from
251   experimental and theoretical studies alike. We find that the experimentally determined fractionation
252   factor for zinc complexation with humic acid [23] is smaller than that for zinc complexation with DMA
253   and the other synthetic ligands studied in this study. Computationally determined fractionation factors
254   for zinc complexation with citrate and malate, thus organic molecules smaller than the ligands studied
255   in this study, show less positive or even negative fractionation [39-41]. Negative fractionation is also
256   observed in computational studies of the complexation of citrate with Ni and Fe [41]. A recently
257   published experimental study of copper complexation with natural and synthetic ligands [29] showed
258   fractionation factors of similar magnitudes for EDTA and for CyDTA, in line with our present work
259   with zinc (Table 3). It is also noteworthy that the isotope fractionation of copper is (i) larger for the
260   complexation with CyDTA than with EDTA and (ii) lower for the complexation with fulvic acid than
261   with synthetic ligands. Both observations seem to hold for Zn (see Table 3 and Jouvin et al., 2009).
262   For Fe, experimental and theoretical studies showed larger fractionation factors during complexation
263   with phytosiderophores and synthetic ligands than with smaller organic ligands such as oxalate or
264   citrate [21, 22, 42]. Table 4 also highlights the disagreement between previous experimental [21] and
265   theoretical [43] studies on the sense of fractionation between Fe-desferrioxamine B (Fe-DFBO) and
266   $Fe(H_2O)_6^{3+}$. Finally, the range of zinc isotope variation observed to date in the terrestrial environment

267   is approximately $\Delta^{66}Zn \sim 1.8‰$ [44] and therefore our data suggests that the extent of fractionation for

268   zinc observed during complexation with phytosiderophores is significant and likely plays a major

269   control of the global biogeochemical cycle of Zn isotopes [45].

270   **Controls of isotope fractionation.** The results for the four hexadentate ligands allow us to

271   explore the link between isotope signatures, reactivity and structure. Despite the similarity in Zn-

272   coordinating donor groups, the differences in the exact geometries of the ZnL^{2-} complexes result in a

273   range of affinity constants ($\log K$) between 12.8 and 18.5 [37, 46] and lead to significantly different isotope

274   fractionation. Figure 3 shows the relationship between $\log K$ and the isotopic fractionation found in

275   our study. There is strong evidence for an increase in heavy bias with increasing complexation

276   strength. This trend has been inferred before by computational studies of organic and inorganic zinc

277   complexes [39]. Similar conclusions were drawn in a theoretical study of organic and inorganic ligands

278   using transition metals including iron, nickel, zinc and copper [41].

279   We obtain the relationship $\Delta^{66}Zn = (0.049 \pm 0.02) \times \log K – (0.366 \pm 0.390)$ ($r^2 = 0.67$, $p = 0.035$).

280   A strong relationship between isotopic fractionation and $\log K$ with organic ligands has been suggested

281   experimentally also for iron [22, 47] and copper [28, 29]. We note that the slope of the linear regression

282   determined for zinc (0.049, this study) and for copper (0.036, [29]) are very similar. While the assessed

283   linear relationship obtained in Figure 3 is affected by the lower value for the EDTA, it is worthwhile

284   to note that the empirical equation predicts negative fractionations for smaller organic molecules such

285   as oxalate, malate and citrate as predicted using calculation before [41] (Table 4).

286   The positive correlation between complexation constant and isotope fractionation observed here

287   may provide a simple empirical tool that may be used to predict fractionation factors for Zn-ligand

288   complexes not yet studied experimentally but relevant to a wide range of biological, medical and

289   environmental relevant ligands.

290   **Comparison with observed isotope fractionation of zinc during plant uptake.** Significant

291   positive isotope fractionation has been observed for zinc uptake by rice grown in paddy soil [4, 5]. The

292   authors tentatively ascribed the heavy isotope bias to uptake of zinc complexed to DMA, consistent

293   with a mathematical modelling exercise [48]. The extent of the heavy isotope fractionation we have

294   determined during zinc complexation by DMA matches the fractionation measure for soil-grown rice [4]

295   as shown in Figure 3. Further work is needed to confirm that rates of DMA secretion by rice under

296   relevant conditions are sufficient to account for enhanced zinc uptake. Further evidence of heavy

297   isotope discrimination during uptake of complexed metals by plants is provided for zinc uptake by

298   tomatoes growing in zinc deficient soil [49], by hyperaccumulators [8, 50], and for iron uptake by

299   phytosiderophore-secreting grasses [14]. Whereas in field and hydroponic studies, Jouvin and co-worker

300   found a light isotopic fractionation of between 0 and -1 ‰ in copper uptake by graminaceous and non-

301   graminaceous plants, suggesting that uptake was not mediated by complexation [12].

302   The findings presented here should make an important contribution to the emerging picture of

303   isotopes as novel technique to study the cycling of zinc and other trace element in the plant-soil

304   environment and to resolve key questions such as mechanisms of zinc uptake in plants.

305

306   **ASSOCIATED CONTENT**

307   **Supporting Information**

308   Further details on the synthesis and characterization of DMA ligand material is available free of
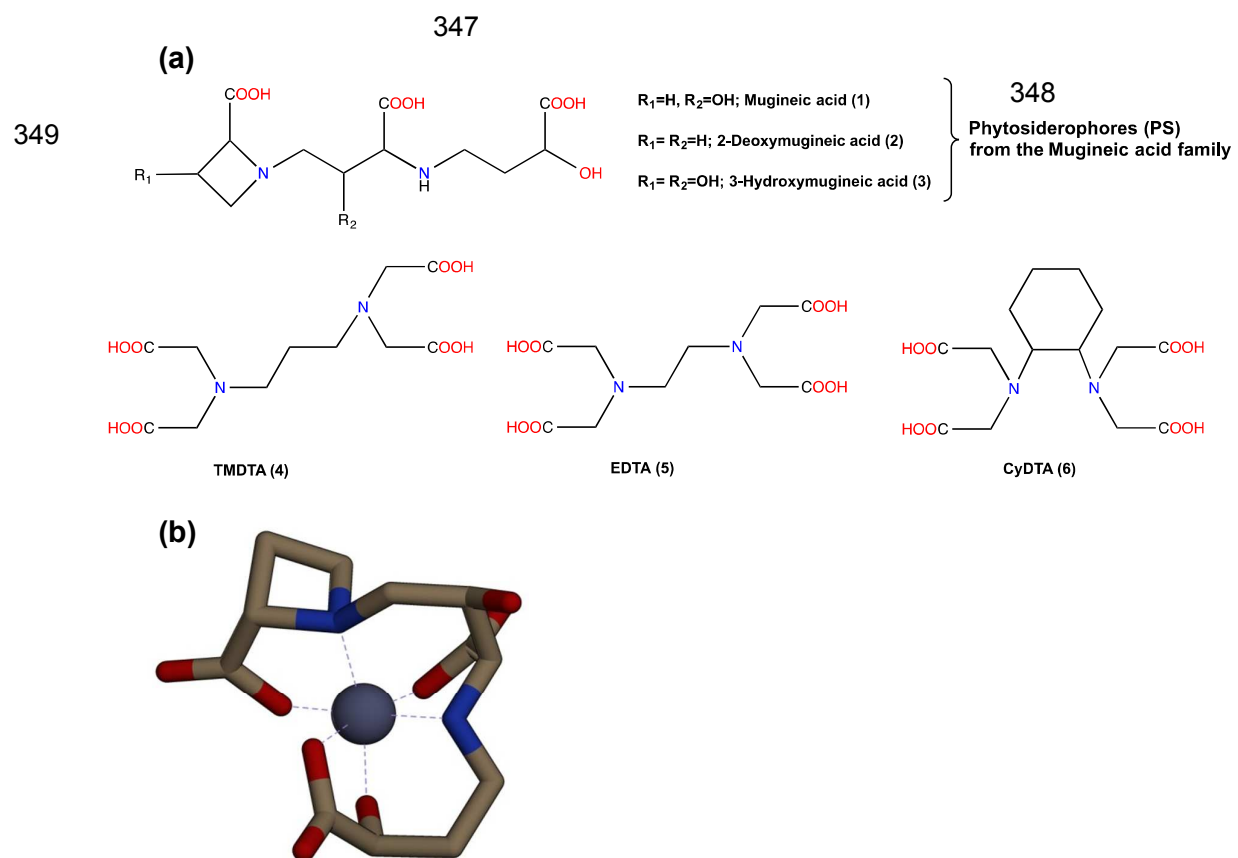309   charge via the Internet at http://pubs.acs.org.

310   **ACKNOWLEDGEMENTS**
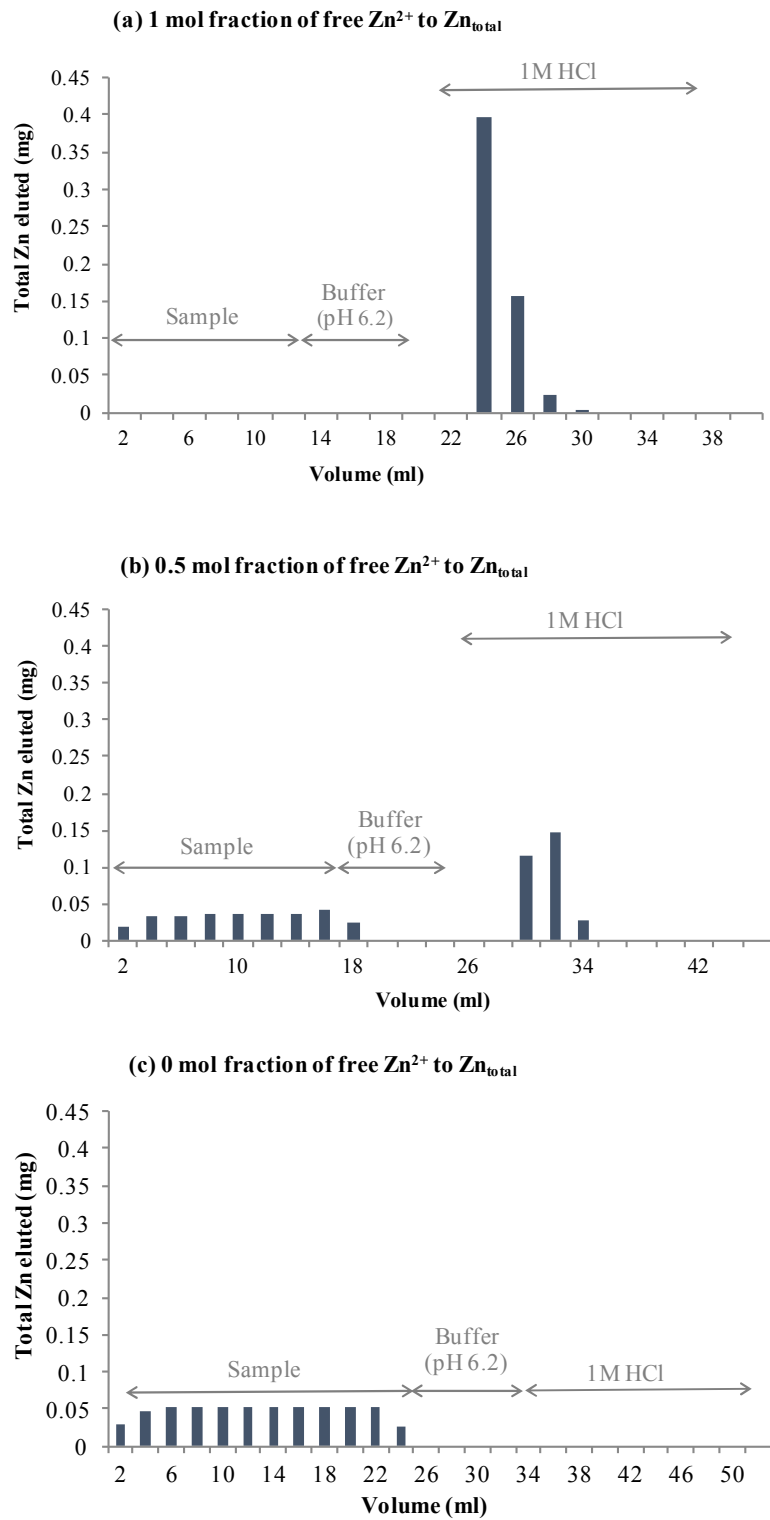
322

323   **Figures**

324   1.   (a) Chemical structures of the four organic ligands tested in this study (**2**, **4-6**), including
325   natural phytosiderophore-ligand from the family of mugineic acids. (b) Molecular
326   structure of the Zn-MA complex modelled with molecular mechanics using ChemBio3D.
327   Note that the colour structures refer to: Zn (iris, central atom), O (red) and N (blue).
328   TmDTA, EDTA and CyDTA coordinate to Zn(II) in an analogous fashion: via the two
329   nitrogen atoms and the four carboxylate groups to give an octahedral complex.

330   2.   Elution profiles of solutions containing different mol fractions (i.e., 1, 0.5, 0) of free Zn^{2+}
331   and complexed $ZnCyDTA^{2-}$ at pH 6.2 (buffered with 0.5 M KMES buffer). (a) 1 mol
332   fraction of free Zn^{2+} to total Zn in the solution shows complete elution of Zn^{2+} in
333   presence of 1 M HCl. (b) 0.5 mole fraction of $ZnCyDTA^{2-}$ is eluted instantly with 0.5 M
334   KMES whereas for eluting free Zn^{2+} fraction 1 M HCl is needed. (c) In 0 mol fraction
335   sample all zinc is eluted instantly in the complexed form. No free Zn^{2+} is present, as
336   visible from the elution profile after addition of 1 M HCl to the columns.

337   3.   Measured and calculated isotopic fractionation of zinc upon complexation by the four
338   organic ligands studied (EDTA, CyDTA, TmDTA and DMA) as a function of the
339   stability constants ($\log K$) of the complex formation [37, 46]. The linear regression is given
340   as y = 0.049±0.02 x - 0.366±0.390, R^2 = 0.6766, p<0.35). Diamonds symbolise $\Delta^{66}Zn$
341   values calculated using measured $\delta^{66}Zn$ for the ZnL^{2-} fraction, crosses symbolise $\Delta^{66}Zn$
342   values calculated using calculated $\delta^{66}Zn$ for the ZnL^{2-} fraction using mass balance
343   considerations. The triangle symbolise the $\Delta^{66}Zn$ values between rice stem and soil
344   solution determined in field experiments in paddy field soils [4]

345

346   Figure 1

347

(a)

349

	R$_1$=H, R$_2$=OH; Mugineic acid (1)	348
	R$_1$= R$_2$=H; 2-Deoxymugineic acid (2)	**Phytosiderophores (PS)**
	R$_1$= R$_2$=OH; 3-Hydroxymugineic acid (3)	**from the Mugineic acid family**

TMDTA (4)   EDTA (5)   CyDTA (6)

(b)

350 Figure 2

(a) 1 mol fraction of free Zn^{2+} to Zn$_{total}$

(b) 0.5 mol fraction of free Zn^{2+} to Zn$_{total}$

(c) 0 mol fraction of free Zn^{2+} to Zn$_{total}$
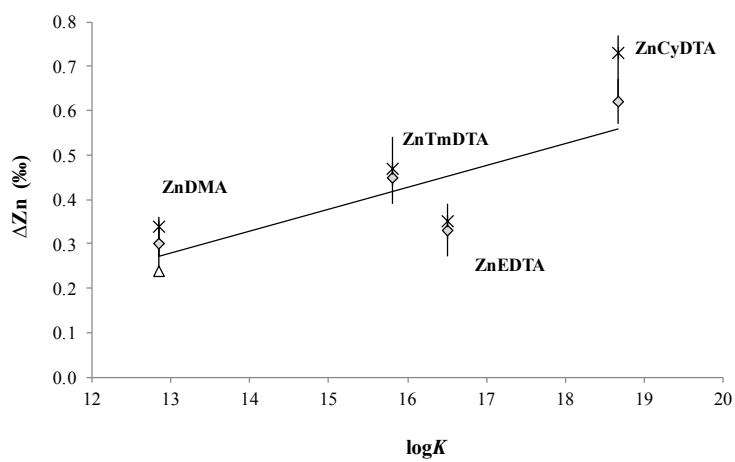
351

352   Figure 3

353

354

355

356 **Tables**

357 1. Protocol for the two different ion exchange procedures used during this study. The
358 cation exchange procedure for the separation of free from complexed zinc used
359 Chelex-100, Amberlite CG50 and Amberlite IR120. The anion exchange
360 chromatography for the removal of spectral and non-spectral interferences derived
361 from the Na-rich matrix for subsequent high precision isotope ratio measurements
362 used AG-MP1

363 2. Separation of free (Zn^{2+}) from complexed (ZnL^{2-}) zinc using the three different resins
364 Chelex-100, Amberlite CG50 and Amberlite IR120. Shown are the affinity constant
365 ($\log K$) for the formation of the relevant complex, the mol fraction of free Zn/total Zn
366 in solutions before and after the passage through the resin, the total amount of zinc
367 loaded onto the resin and the amount of zinc eluted from the resin after passage
368 through column

369 3. Experimentally determined $\delta^{66}Zn$-value for free Zn^{2+} and for complexed ZnL^{2-}
370 fractions in solutions with different mol fractions (expressed as $f_{Zn} = Zn^{2+}/Zn_{total}$). The
371 $\delta^{66}Zn$-value of the complexed ZnL^{2-} fraction was also calculated using mass balance
372 constraints. (See text for details). The experimental fraction factor for the
373 complexation of Zn^{2+} with ZnL^{2-} was calculated for each solution using $\Delta^{66}Zn =$
374 $\delta^{66}Zn_{ZnL2-} - \delta^{66}Zn_{Zn2+}$ and then averaged for each Zn^{2+}/ZnL^{2-} system using the
375 available $\Delta^{66}Zn$ values (the mean is shown in bold, n indicates the number of $\Delta^{66}Zn$
376 values used, $\pm 1SD$ indicates the standard deviation). Also shown are recoveries of the
377 ion exchange procedure and the amount of zinc loaded upon the resin and collected
378 afterwards.

379 4. Published fractionation factors of transition row metals during complexation with
380 organic ligands using laboratory experiments and theoretical calculations. The
381 fractionation is expressed using Δ-values in per mill per atomic mass unit, i.e., $\Delta^{x/y}M$
382 $= (\delta^{x/y}ML^{2-} - \delta^{x/y}M^{2+}) / (x-y)$, where x and y are two different isotopes (x = heavy and
383 y = light), M is the metal studied and δ is the small delta value for free (M^{2+}) and
384 complexed (ML^{2-}) species. DFBO = desferrioxamine B, PHA = purified humic acid,
385 IHA = insolubilized humic acid, EDTA = ethylenediaminetetraacetic acid, TmDTA =
386 trimethylenedinitrilotetraacetic acid, CyDTA = cyclohexanediaminetetraacetic acid

387

388   Table 1

Ion exchange procedure	Objective	Resin	System studied	Step	Medium	Volume ml
Cation Exchange	To separate free Zn^{2+} from complexed ZnL^{2-}	Chelex-100, Na^+ form, 200-400 mesh	Zn/ZnEDTA	Resin Loading	H_2O	1 - 2
			Zn/ZnCyDTA	Cleaning	2M HCl	5 x 2
				Conditioning	H_2O	3 x 2
		Amberlite CG50, H^+ form, 100-200 mesh	Zn/ZnTmDTA	Equilibration	KMES buffer (pH 6.2)	3 x 2
				Sample loading	H_2O (pH 6.3)	5 x 2 up to 10 x 2
				Matrix elution	KMES buffer (pH 6.2)	2 x 2
		Amberlite IR120, H^+ form	Zn/ZnDMA		H_2O	3 x 2
				Zn2+ fraction	1M HCl	5 x 2
				Cleaning	1M NaOH	2 x 2
					H_2O	3 x 2
Anion Exchange	To remove isobaric and non isobaric interferences	AG MP1, BioRad, Cl^- from, 100-200 mesh		Resin Loading	0.5M HNO_3	1 - 2
				Cleaning	0.5M HNO_3	5 x 6
				Conditioning	H_2O	5 x 3
					6M HCl	4 x 1
				Sample loading	6M HCl	1 x 1
				Matrix elution	6M HCl	3 x 3
					2M HCl	2 x 3.5
				Zn elution	0.1M HCl	2 x 3.5
				Cleaning	0.5M HNO_3	5 x 2
					H_2O	5 x 1

389
390

391 Table 2

Ligand	$\log K$	Resin	Before column		After column			Dissociation of complex
			Mol fraction targeted Zn^{2+}/Zn_{total}	Total Zn added	ZnL^{2-} - fraction	Zn^{2+} fraction	Mol fraction effective Zn^{2+}/Zn_{total}	
			-	mg	mg	mg	-	
CyDTA	18.5	Chelex-100	1.00	0.580	0.000	0.580	1.00	
			0.50	0.580	0.289	0.291	0.50	No
			0.00	0.580	0.580	0.000	0.00	No
EDTA	16.4	Chelex-100	1.00	0.463	0.000	0.463	1.00	
			0.50	0.555	0.258	0.297	0.53	No
			0.00	0.530	0.518	0.013	0.02	No
TmDTA	15.6	Chelex-100	1.00	0.610	0.000	0.610	1.00	
			0.50	0.622	0.131	0.492	0.79	Partial
			0.00	0.662	0.235	0.426	0.64	Partial
		Amberlite CG50	0.50	0.380	0.168	0.212	0.56	No
			0.00	0.371	0.328	0.044	0.12	No
DMA	12.8	Amberlite CG50	0.50	0.266	0.010	0.256	0.96	Full
			0.00	0.267	0.019	0.248	0.93	Full
		Amberlite IR120	0.50	0.190	0.127	0.062	0.33	Possible
			0.00	0.204	0.175	0.029	0.14	Possible

392

393

16

394   Table 3

Ligand	Sample ID	Fractions Zn^{2+} mass mg	mol fraction	δ^{66} Zn per mill	±2SD	ZnL^{2-} mass mg	mol fraction	δ^{66} Zn measured per mill	±2SD	δ^{66} Zn calculated per mill	Δ-value measured per mill	calcuated per mill	n	Mass balance Zn added mg	Zn eluted mg	Recovery %
EDTA	Stock Solution							-0.06								
	1	0.114	0.20	-0.33	0.07	0.47	0.80	n.d.	n.d.	0.01	n.d.	0.34		0.583	0.582	100
	2	0.488	1.00	0.04	0.03	0.000	0.00	n.d.	n.d.	n.d.	n.d.	n.d.		0.583	0.488	84
	3	0.157	0.27	-0.33	0.08	0.421	0.73	0.07	0.00	0.04	0.40	0.37		0.583	0.579	99
	4	0.249	0.43	-0.27	0.07	0.327	0.57	0.07	0.03	0.10	0.34	0.38		0.583	0.576	99
	5	0.398	0.70	-0.15	0.06	0.174	0.30	0.10	0.04	0.16	0.26	0.31		0.583	0.572	98
	6	0.564	1.00	-0.04	0.01	0.00	0.00	n.d.	n.d.	n.d.	n.d.	n.d.		0.583	0.564	97
	mean										**0.33**	**0.35**	**3**			
	± 1SD										**0.07**	**0.04**				
TmDTA	Stock Solution							0.09								
	7	0.026	0.03	-0.31	0.05	0.774	0.97	0.12	0.07	0.10	0.43	0.41		0.739	0.800	108
	8	0.270	0.35	-0.25	0.11	0.505	0.65	0.21	0.18	0.27	0.46	0.53		0.739	0.775	105
	mean										**0.45**	**0.47**	**2**			
	± 1SD										**0.02**	**0.08**				
CyDTA	Stock Solution							0.01								
	9	0.003	0.01	n.d.	n.d.	0.545	0.99	n.d.	n.d.	n.d.	n.d.	n.d.		0.583	0.548	94
	10	0.086	0.16	-0.50	0.16	0.453	0.84	0.06	0.01	0.11	0.57	0.61		0.583	0.539	92
	11	0.456	1.00	-0.01	0.1	0.000	0.00	n.d.	n.d.	n.d.	n.d.	n.d.		0.583	0.456	78
	12	0.002	0.00	n.d.	n.d.	0.613	1.00	-0.02	0.00	n.d.	n.d.	n.d.		0.583	0.615	105
	13	0.109	0.20	-0.62	0.02	0.437	0.80	0.04	0.02	0.17	0.66	0.79		0.583	0.546	94
	14	0.266	0.48	-0.40	0.02	0.283	0.52	0.23	0.00	0.39	0.62	0.79		0.583	0.550	94
	15	0.528	1.00	0.05	0.01	0.000	0.00	n.d.	n.d.	n.d.	n.d.	n.d.		0.583	0.528	91
	mean										**0.62**	**0.73**	**3**			
	± 1SD										**0.05**	**0.10**				
DMA	Stock Solution							0.01								
	16	0.133	0.31	-0.23	0.07	0.300	0.69	0.13	0.01	0.12	0.36	0.34		0.414	0.434	105
	17	0.203	0.53	-0.16	0.06	0.179	0.47	0.07	0.03	0.21	0.24	0.37		0.414	0.382	92
	18	0.142	0.35	-0.21	0.01	0.258	0.65	0.15	0.06	0.13	0.36	0.34		0.414	0.400	97
	19	0.216	0.57	-0.12	0.09	0.165	0.43	0.13	0.03	0.18	0.26	0.31		0.414	0.381	92
	mean										**0.30**	**0.34**	**4**			
	± 1SD										**0.07**	**0.03**				

395

17

396 Table 4

Element	Complexation reaction	Isotope Fractionation per mill per atomic mass unit	Comment		Reference
Iron	$Fe^{3+} + DFOB^{4-} = [Fe(DFOB)]^-$	0.3	Experimental	Phase separation	Dideriksen et al., 2008
	$Fe^{3+} + DFOB^{4-} = [Fe(DFOB)]^-$	>0	Experimental	Membrane separation	Morgan et al., 2010
	$Fe^{3+} + DFOB^{4-} = [Fe(DFOB)]^-$	-0.2	Ab initio calculations	DFT theory	Domagal-Goldman et al., 2009
	$Fe^{3+} + (citrate)_2^{6-} = [Fe(citrate)_2]^{3-}$	-0.4	Ab initio calculations	DFT theory	Fujii et al. 2014
	$Fe^{2+} + (citrate)_2^{6-} = [Fe(citrate)_2]^{4-}$	-0.6	Ab initio calculations	DFT theory	Fujii et al. 2014
	$Fe^{2+} + Nicotinamine^{4+} = [Fe(Nicotinamine)]^{2-}$	-0.03	Ab initio calculations	DFT theory	Moynier et al., 2013
	$Fe^{3+} + Phytosiderophore^{3-} = [Fe(Phytosiderophore)]^0$	0.5	Ab initio calculations	DFT theory	Moynier et al., 2013
Zinc	$Zn^{2+} + PHA^{n-} = [Zn(PHA)]^{m-}$	0.1	Experimental	Membrane separation	Jouvin et al., 2009
	$Zn^{2+} + citrate^{3-} = [Zn(citrate)]^-$	0.07 to 0.25	Ab initio calculations	DFT theory	Black et al., 2011
	$Zn^{2+} + [citrate(H_2O)_3]^{3-} = [Zn(citrate(H_2O)_3)]^-$	0.1	Ab initio calculations	DFT theory	Fujii and Albarede, 2012
	$Zn^{2+} + (citrate)_2^{6-} = [Zn(citrate)_2]^{4-}$	-0.4	Ab initio calculations	DFT theory	Fujii and Albarede, 2012
	$Zn^{2+} + [malate(H_2O)_4]^{2-} = [Zn(malate(H_2O)_4)]^0$	0.1	Ab initio calculations	DFT theory	Fujii and Albarede, 2012
	$Zn^{2+} + [(malate)_2(H_2O)_2]^{4+} = [Zn(malate)(H_2O)_n]^{m-}$	-0.2	Ab initio calculations	DFT theory	Fujii and Albarede, 2012
Nickel	$Ni^{2+} + (citrate)_2^{6-} = [Fe(citrate)_2]^{4+}$	-0.6	Ab initio calculations	DFT theory	Fujii et al. 2014
Copper	$Cu^{2+} + IHA^{n-} = [Zn(IHA)]^{m-}$	0.1	Experimental	Membrane separation	Bigalke et al, 2010
	$Cu^{2+} + DFOB^{4+} = [Cu(DFOB)]^{2-}$	0.42	Experimental	Membrane separation	Ryan et al., 2014
	$Cu^{2+} + CyDTA^{4-} = [Cu(CyDTA)]^{2-}$	0.31	Experimental	Membrane separation	Ryan et al., 2014
	$Cu^{2+} + EDTA^{4+} = [Cu(EDTA)]^{2-}$	0.25	Experimental	Membrane separation	Ryan et al., 2014
	$Cu^{2+} + Nitrilotriacetic\ acid^{3-} = [Cu(Nitrilotriacetic\ acid)]^-$	0.22	Experimental	Membrane separation	Ryan et al., 2014
	$Cu^{2+} + Fulvic\ acid^{n-} = [Cu(Fulvic\ acid)]^{m-}$	0.07	Experimental	Membrane separation	Ryan et al., 2014

397

18

398   **TOC/ Abstract art**

399

400

401

402

403
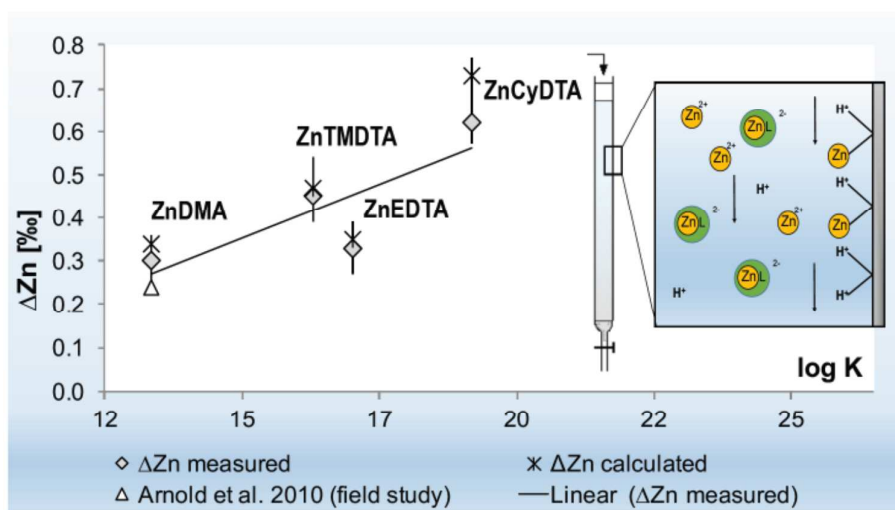
REFERENCES

405

406   1. Wiederhold, J. G., Metal stable isotope signatures as tracers in environmental
407   geochemistry. *Environ. Sci. Technol.* **2015,** *49*, (5), 2606-2624.
408   2. von Blankenburg, F.; Von Wiren, N.; Guelke, M.; Weiss, D. J.; Bullen, T. D., Metal
409   stable isotope fractionation by higher plants. *Elements* **2009,** *5*, (6), 375-380.
410   3. Weiss, D. J.; Mason, T. F. D.; Zhao, F. J.; Kirk, G. J. D.; Coles, B. J.; Horstwood, M. S.
411   A., Isotopic discrimination of Zn in higher plants. *New Phytol.* **2005,** *165*, 703-710.
412   4. Arnold, T.; Kirk, G. J. D.; Wissuwa, M.; Frei, M.; Zhao, F. J.; Weiss, D. J., Evidence for
413   the mechanisms of zinc efficiency in rice using isotope discrimination. *Plant Cell Environ.*
414   **2010,** *33*, 370-381.
415   5. Arnold, T.; Markovic, T.; Guy, K.; Schoenbachler, M.; Rehkamper, M.; Zhao, F.; Weiss,
416   D., Iron and zinc isotope fractionation during uptake and translocation in rice (Oryza sativa)
417   grown in oxic and anoxic soils. *C. R. Geoscience* **2015,** *347*, 397–404.
418   6. Houben, D.; Sonnet, P.; Tricot, G.; Mattielli, N.; Couder, E.; Opfergelt, S., Impact of
419   Root-Induced Mobilization of Zinc on Stable Zn Isotope Variation in the Soil–Plant System.
420   *Environmental science & technology* **2014,** *48*, 7866-7873.
421   7. Couder, E.; Mattielli, N.; Drouet, T.; Smolders, E.; Delvaux, B.; Iserentant, A.; Meeus,
422   C.; Maerschalk, C.; Opfergelt, S.; Houben, D., 2015.. , Transpiration flow controls Zn
423   transport in Brassica napus and Lolium multiflorum under toxic levels as evidenced from
424   isotopic fractionation. *Comptes Rendus Geoscience* **2015,** *347*, 386-396.
425   8. Tang, Y.-T.; Cloquet , C.; Sterckeman, T.; Echevarria, G.; Carignan , J.; Qiu, R.-L.;
426   Morel, J.-L., Fractionation of stable zinc isotopes in the field-grown zinc hyperaccumulator
427   noccaea caerulescens and the zinc-tolerant plant silene vulgaris. *Environ. Sci. Technol.* **2012,**
428   *46*, (18), 9972–9979.
429   9. Viers, J.; Oliva, P.; Nonell, A.; Gélabert, A.; Sonke, J. E.; Freydier, R.; Gainville, R.;
430   Dupré, B., Evidence of Zn isotopic fractionation in a soil–plant system of a pristine tropical
431   watershed (Nsimi, Cameroon). *Chem. Geol.* **2007,** *239*, 124–137.
432   10. Aucour, A. M.; Pichat, S.; Macnair, M. R.; Oger, P., Fractionation of stable zinc isotopes
433   in the zinc hyperaccumulator Arabidopsis halleri and nonaccumulator Arabidopsis petraea.
434   *Environ. Sci. Technol.* **2011,** *45*, (21), 9212-9217.
435   11. Deng, T.; Cloquet , C.; Tang, Y.-T.; Sterckeman, T.; Echevarria, G.; Estrade, N.; Morel,
436   J.-L.; Qiu, R.-L., Nickel and zinc isotope fractionation in hyperaccumulating and
437   nonaccumulating plants. *Environ. Sci. Technol.* **2014,** *48*, 11926-11933.
438   12. Jouvin, D.; Weiss, D. J.; Mason, T. F.; Bravin, M. N.; Louvat, P.; Zhao, F.; Ferec, F.;
439   Hinsinger, P.; Benedetti, M. F., Stable isotopes of Cu and Zn in higher plants: evidence for Cu
440   reduction at the root surface and two conceptual models for isotopic fractionation processes.
441   *Environmental science & technology* **2012,** *46*, (5), 2652-60.
442   13. Bigeleisen, J.; Mayer, M. G., Calculation of equilibrium constants for isotopic exchange
443   reactions. *J. Chem. Phys.* **1947,** *15*, 261-267.
444   14. Guelke, M.; von Blankenburg, F., Fractionation of stable iron isotopes in higher plants.
445   *Environ. Sci. Technol.* **2007,** *41*, (6), 1896-1901.
446   15. Suzuki, M.; Takahashi, M.; Tsukamoto, T.; S., W.; Matsuhashi, S. Y., J.; Kishimoto, N.;
447   Kikuchi, S.; Nakanishi, H.; Mori, S.; Nishizawa, N. K., Biosynthesis and secretion of
448   mugineic acid family phytosiderophore in zinc-deficient barley. *Plant J.* **2006,** *48*, 85-97.
449   16. Suzuki, M.; Tsukamoto, T.; Inoue, H.; S., W.; Matsuhashi, S.; Takahashi, M.; Nakanishi,
450   H.; Mori, S.; Nishizawa, N. K., Deoxymugeneic acid increases Zn translocation in Zn
451   deficient rice plants. *Plan Mol Biol* **2008,** *66*, 609-617.
452   17. Hacisalihoglu, G.; Kochian, L. V., How do some plants tolerate low levels of soil zinc?
453   Mechanisms of zinc efficiency in crop plants. *New Phytol.* **2003,** *159*, (2), 341-350.
454   18. Tagaki, S., Naturally occuring iron compounds in oat and rice root washings: 1. Activity
455   Measurement and Preliminary Characterization. *Soil Sci. Plant Nutr.* **1976,** *22*, (4), 423-433.

456   19. Namba, K.; Murata, Y.; Horikawa, M.; Iwashita, T.; Kusumoto, S., A practical synthesis
457   of the phytosiderophore 2'-deoxymugineic acid : a key to the mechanistic study of iron
458   acquisition by graminaceous plants. *Angew Chem Int Ed Engl* **2007,** *46*, (37), 7060-7063.
459   20. Walter, M. R.; Artner, D.; Stanetty, C., Synthesis of [13C4]-labeled 2'-deoxymugineic
460   acid. *J Labelled Comp Radiopharm* **2014,** *57*, (13), 710-714.
461   21. Dideriksen, K.; Baker, J. A.; Stipp, S. L. S., Equilibrium Fe isotope fractionation between
462   inorganic aqueous Fe(III) and the siderophore complex, Fe(III)-desferrioxamine B. *Earth
463   Planet. Sci. Lett.* **2008,** *269*, 280-290.
464   22. Morgan, J. L. L.; Wasylenki, L. E.; Nusester, J.; Anbar, A. D., Fe Isotope Fractionation
465   during Equilibration of Fe-Organic Complexes. *Environmental Science Technology* **2010,** *44*,
466   6095-6101.
467   23. Jouvin, D.; Louvat, P.; Juillot, F.; Marechal, C.; Benedetti, M., Zinc isotopic
468   fractionation: why organic matters. *Environ Sci Technol.* **2009,** *43*, 5747-5754.
469   24. Weng, L.; Alonso Vega, F.; Van Riemsdijk, W., Strategies in the application of the
470   Donnan membrane technique. *Environ Chem* **2011,** *8*, (5), 466-474.
471   25. Pesavento, M.; Biesuz, R.; Cortina, J. L., Sorption of metal ions on a weak acid cation
472   exchange resin containing carboxalicgroups. *Anal Chem Acta* **1994,** *298*, (2), 225-232.
473   26. Criss, R. E., *Principles of stable isotope distribution*. Oxford University Press: Oxford,
474   1999.
475   27. Johnson, C. M.; Beard, B. L.; Albarède, F., Overview and General Concepts. In
476   *Geochemistry of non-traditional stable isotopes*, Johnson, C. M.; Beard, B. L.; Albarède, F.,
477   Eds. Mineralogical Society of America: 2004; Vol. 55, pp 1-22.
478   28. Bigalke, M.; Weyer, S.; Wilcke, W., Copper isotope fractionation during complexation
479   with insolubilized humic acid. *Environ. Sci. Technol.* **2010,** *44*, 5496-5502.
480   29. Ryan, B. M. K.; Degryse, F.; Scheiderich, K.; McLaughiln, M. J., Copper Isotope
481   Fractionation during Equilibrium with Natural and Sythetic Ligands. *Env. Sci. Technol.* **2014,**
482   *48*, 8620-8626.
483   30. Bowles, K. C.; Apte, S. C.; Batley, G. E.; Hales, L. T.; Rogers, N. J., A rapid Chelex
484   column method for the determination of metal speciation in natural waters. *Anal Chim Acta*
485   **2006,** *558*, 237–245.
486   31. Shaff, J. E.; Schultz, B. A.; Craft, E. J.; Clark, R. T.; Kochian, L. V., GEOCHEM-EZ: a
487   chemical speciation program with greater power and flexibility. *Plant Soil* **2009,** *330*, 207-
488   214.
489   32. Peel, K.; Weiss, D. J.; Chapman, J.; Arnold, T.; Coles, B. J., A simple combined sample-
490   standard bracketing and inter-element correction procedure for accurate and precise Zn and Cu
491   isotope ratio measurements. *J. Anal. At. Spectrom.* **2007,** *22*, 1-8.
492   33. Kingston, H. M.; Barnes, I. L.; Brady, T. J.; Rains, T. C.; Champ, M. A., Separation of
493   eight transition elements from alkali and alkaline earth elements in estuarine and seawater
494   with chelating resin and their determination by graphite furnace atomic absorption
495   spectrometry. *Anal. Chem.* **1978,** *50*, 2064-2070.
496   34. Dong, S.; Weiss, D. J.; Strekopytov, S.; Kreissig, K.; Sun, Y.; Baker, A. R.; Formenti, P.,
497   Stable isotope ratio measurements of Cu and Zn in mineral dust (bulk and size fractions) from
498   the Taklimakan Desert and the Sahel and in aerosols from the eastern tropical North Atlantic
499   Ocean. *Talanta* **2013,** *114*, 103-109.
500   35. Arnold, T.; Schonbachler, M.; Rehkamper, M.; Dong, S.; Zhao, F. J.; Kirk, G. J.; Coles,
501   B. J.; Weiss, D. J., Measurement of zinc stable isotope ratios in biogeochemical matrices by
502   double-spike MC-ICPMS and determination of the isotope ratio pool available for plants from
503   soil. *Anal. Bioanal. Chem.* **2010,** *398*, (7-8), 3115-25.
504   36. Moeller, K.; Schoenberg, R.; Pedersen, R.; Weiss, D. J.; Dong, S., Calibration of the new
505   certified isotopic reference materials ERM-AE647 (Cu) and IRMM-3702 (Zn) against the
506   previously used NIST SRM 976 (Cu) and 'JMC Lyon' (Zn) solutions – A new reference scale
507   for copper and zinc isotope determinations. *Geostand. Geoanal. Res.* **2011,** *36*, 177-199.
508   37. Bjerrum, J.; Schwarzenbach, G.; Sillen, L. G., *Stability Constants*. Chemical Society,
509   London: 1958.

510 38. Weiss, D. J.; Harris, C.; Maher, K.; Bullen, T., A Teaching Exercise To Introduce Stable
511 Isotope Fractionation of Metals into Geochemistry Courses. *J. Chem. Edu.* **2013,** *90*, (8),
512 1014-1017.
513 39. Black, J. R.; Kavner, A.; Schauble, E. A., Calculation of equilibrium stable isotope
514 partition function ratios for aqueous zinc complexes and metallic zinc. *Geochim. Cosmochim.*
515 *Acta* **2011,** *75*, (3), 769 - 783
516 40. Fujii, T.; Albarède, F., Ab initio calculation of the Zn isotope effect in phosphates,
517 citrates, and malates and applications to plants and soil. *PLoS ONE* **2012,** *7*, (2),
518 doi:10.1371/journal.pone.0030726.
519 41. Fujii, T.; Moynier, F.; Blichert-Toft, J.; Albarede, F., Density functional theory estimation
520 of isotope fractionation of Fe, Ni, Cu and Zn among species relevant to geochemical and
521 biological environments. *Geochim. Cosmochim. Acta* **2014,** *140*, 553-576.
522 42. Moynier, F.; Fujii, T.; Wanga, K.; Foriel, J., Ab initio calculations of the Fe(II) and
523 Fe(III) isotopic effects in citrates, nicotianamine,and phytosiderophore,and new Fe isotopic
524 measurements in higher plants. *Comptes Rendues Geosci.* **2013**.
525 43. Domagal-Goldman, S. D.; Paul, K. W.; Sparks, D. L.; Kubicki, J. D., Quantum chemical
526 study of the Fe(III)-desferrioxamine B siderophore complex—Electronic structure, vibrational
527 frequencies, and equilibrium Fe-isotope fractionation. *Geochim. Cosmochim. Acta* **2009,** *73*,
528 (1), 1-12.
529 44. Cloquet, C.; Carignan, J.; Lehmann, M. F.; Vanhaecke, F., Variations in the isotopic
530 composition of zinc in the natural environment and the use of zinc isotopes in biogeosciences:
531 a review. *Anal. Bioanal. Chem.* **2008,** *390*, 451-463.
532 45. Little, S. H.; Vance, D.; Walker-Brown, C.; Landing, W. M., The oceaninc mass balance
533 of copper and zinc isotopes, investigated by analysis of their inputs, and outputs to
534 ferrommanganese oxide sediments. *Geochim. Cosmochim. Acta* **2014,** *125*, 673-693.
535 46. Murakami, T.; Ise, K.; Hayakawa, M.; Kamei, S.; Takagi, S., Stabilities of metal
536 complexes of mugineic acids and their specific affinities for iron(III). *Chem. Lett.* **1989**, 2137-
537 2140.
538 47. Brantley, S. L.; Liermann, L.; Bullen, T. D., Fractionation of Fe isotopes by soil microbes
539 and organic acids. *Geology* **2001,** *29*, (6), 535-538.
540 48. Ptashnyk, M.; Roose, T.; Jones, D. L.; Kirk, G. J. D., Enhanced zinc uptake by rice by
541 phytosiderophore secretion: a modelling study. *Plant, Cell Enviro.* **2011,** *34*, (12), 2038–2046.
542 49. Smolders, E.; Versieren, L.; Dong, S.; Mattielli, N.; Weiss, D. J.; Petrov, I.; Degryse, F.,
543 Isotopic fractionation of Zn in tomato plants reveals the role of root exudates on Zn uptake
544 *Plant Soil* **2013,** *370*, (1-2), 605-613.
545 50. Caldelas, C.; Dong, S.; Araus, J. L.; Weiss, D. J., Zinc isotopic fractionation in
546 *Phragmites australis* in response to toxic levels of zinc. *J. Exp. Bot.* **2011,** *62*, (6), 2169-78.

547